MXenes: Two-Dimensional Futuristic Material

Uday Karanbir Singh[1]*, Harpreet Kaur[1], Taranveer Kaur[1], Pushpinder Kaur[2], Richa Rastogi[1]*

[1]Centre for Nanoscience & Nanotechnology, Panjab University, Chandigarh.

[2]Department of Chemistry, Sri Guru Gobind Singh College, Sector-26, Chandigarh

Corresponding author E-mail id: sainiuday1@gmail.com, richa.bend@gmail.com

1. INTRODUCTION

The rapidly expanding group of nanostructured materials includes two-dimensional (2D) layered materials, which have distinctive physical and chemical properties. These materials have seen a wide range of applications in recent years [1]. 2D materials are specifically characterized by one dimension being restricted to a single atom or just a few atoms (less than 5 nm), while the other dimensions can reach up to 100 nm or a few micrometers [1] – [3].

A notable addition to this category is MXenes, which have gathered significant attention since their discovery [4]. MXenes belong to a new group of transition essence carbides, nitrides, or carbonitrides, flaunting unique morphology and exceptional parcels applicable to different fields similar as energy storehouse, gas sensing, electromagnetic hindrance (EMI) shielding, and membrane-grounded water filtration [5]. These MXenes are typically produced through the chemical delamination of three-dimensional (3D) ternary or quaternary compounds known as MAX phases. The formula for MAX phases is $M_{n+1}AX_n$ (n = 1, 2, or 3), where M represents an early transition metal such as Ti, Nb, V, Mo, Ta, Cr, Hf, Zn, or Sc, X denotes carbon (C) and/or nitrogen (N), and A consists of elements from groups 13 and 14 in the periodic table [6]. MAX phases are

technologically significant materials due to their intriguing combination of metallic and ceramic characteristics [7].

MXenes are typically produced through a selective chemical etching process that removes A layers from their parent MAX-phase precursors. Currently, more than 30 different MXenes have been successfully synthesized, and several others have been predicted theoretically [8]. The general formula for MXenes is given as $M_{n+1}X_nT_n$ or $M_{1.33}XT_n$, with M representing an early transition metal, X denoting C and/or N, and T indicating the surface terminal group (O, F, or OH) [9]. Depending on the value of n in MAX phases, the resulting MXenes can have M_2X, M_3X_2, or M_4X_3 lattice structures [10], as shown in Fig.1. MXenes possess a layered structure where the single surface group terminated MX layers are stacked. The stacking types of MX layers, namely simple hexagonal (SH) and Bernal stacks are determined by the relative position of the layers with terminations. These layers are connected through dihydrogen bonding between the surface groups, while the intralayers are held together by strong covalent and ionic bonds.

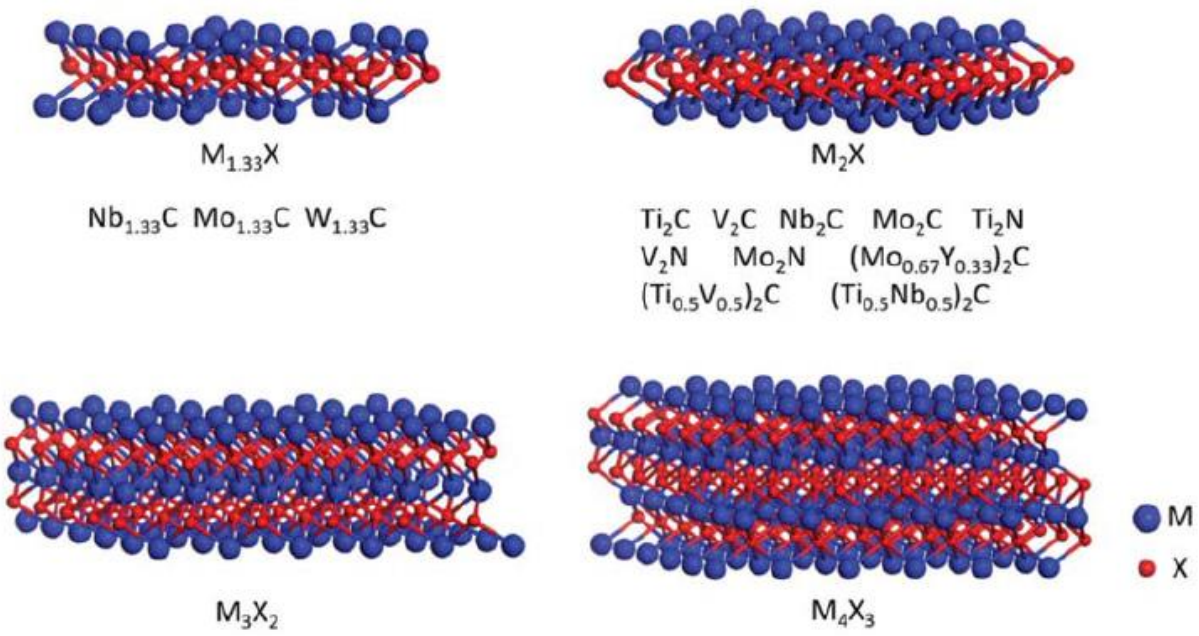

Fig 1. Illustration of schematics depicting an overview of experimentally synthesized MXenes. Reproduced with permission from ref. [110], copyright 2020, Nanophotonics.

MXenes are characterized by multiple M elements and two types of structures: solid solutions and ordered phases (Fig.2). Solid solutions refer to the random arrangement of two individual or separate transition metals in M layers, while ordered phases involve a monolayer or double layers of a single transition metal with the first transition metal intercalated between the layers of the second transition metal in the 2D carbide structure [11]. The properties of MXenes, including their electronic and optical characteristics, are closely linked to M elements and T surface functional groups. The combination of features exhibited by MXenes is remarkable, such as 2D surface morphology, metallic conductivity, high surface area, excellent flexibility, mechanical strength, and hydrophilicity [12]. The metallic conductivity arises from the presence of free electrons in transition metal carbides or nitrides, while the hydrophilicity is a result of the surface terminations. The diverse range of transition metals, along with different surface functionalities, allows for the tuning of MXene properties. Consequently, MXenes possess versatile and rich surface chemistry, making them suitable for potential applications in various research fields.

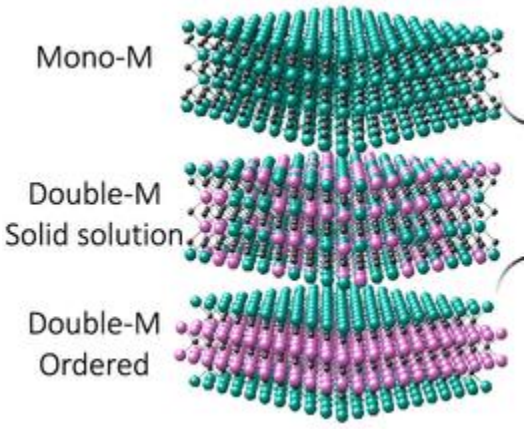

Fig 2. MXenes can be of three different forms: (a) mono-M elements (For example Ti_2C) (b) solid solution where at least two different M elements (for example $(Ti,V)_3C_2$(c) ordered double-M elements in which one transition metal occupies perimeter layers and other fills the central M layer (for example Mo_2TiC_2, in which outer M layer are Mo and central M layer are Ti). Reproduced from permission from ref.[111] , copyright 2021, ACS nano.

2. STRUCTURE AND PROPERTIES OF MXENES

2.1. Structure of MXene: -

The synthesis of MXenes primarily involves wet etching of MAX phases. In MAX phases, the M atoms are arranged in a hexagonal close-packed (hcp) structure, with the X atoms occupying the octahedral interstices. These interstices are interleaved with layers of A-group elements in the $P6_3/mmc$ space group [13]. Once the A layers are removed, the remaining $M_{n+1}X_n$ layers form a 2D hexagonal close-packed structure, with the addition of O, OH, F, H, and/or Cl atoms. MXenes are always fully terminated, as evidenced by their higher negative formation energy when surface terminations bond with the outer transition metal layers [14], as well as positive phonon frequencies [15] observed in fully terminated MXenes. Different configurations are possible for functional group terminations in MXenes. Three major types are considered (Fig. 3a): type I, where functional groups are positioned above the hollow sites of three neighboring X atoms and directed towards the M atoms in the second Ti atomic layer; type II, where functional groups are located on top of the topmost sides of the X atoms; and type III, which is a combination of types I and II, with one functional group above the hollow sites of the X atoms on one side and another functional group above the top sites of the X atoms on the other sides. Theoretical calculations indicate that type I configuration is the most stable for the majority of MXenes [13] – [15].

The conductivity of MXenes is influenced by the anisotropy resulting from the strong intralayer bonding and weak interlayer bonding, which is 2-6 times larger than that of well-known 2D materials like graphite and MoS_2. The interlayer coupling needs to be weakened for successful exfoliation into monolayers, but the relatively stronger interlayer bonding ensures the stability of the layered structure during reversible electrochemical intercalation reactions.

Functional groups play crucial roles in MXenes' applications, such as energy storage. However, there is a discrepancy between theoretical predictions and experimental results due to the simplified models used in theoretical studies. The functionalization of MX layers involves a spontaneous and competitive adsorption process, resulting in a coexisting feature of terminations that maximizes entropy. Among the functional groups, -O terminations are more stable due to their stronger covalent bonding with the transition metal in the MX layer [16].

As shown in Fig 3(c), The HF-etched MXene exhibits a layered structure with a *c* lattice parameter of 19.8 Å [17], and the high-angle annular dark-field scanning transmission electron microscopy (HAADF-STEM) images show a non-uniform interlayer spacing. The interlayer interactions between different terminations lead to inhomogeneous interlayer spacing and imply the coexistence of functional groups. Intercalation of cations or annealing in ammonia can improve the homogeneity of layered domains. STEM images and XRD patterns confirm the changes in interlayer spacing and crystallinity after intercalation or annealing.

MXenes are not structurally perfect and exhibit point defects, such as Ti vacancies caused by the etching process. The concentration of vacancies can be controlled by the etchant concentration [18]. Point defects, including vacancies and adatoms, offer opportunities to control the surface properties of MXenes for energy storage and catalytic applications.

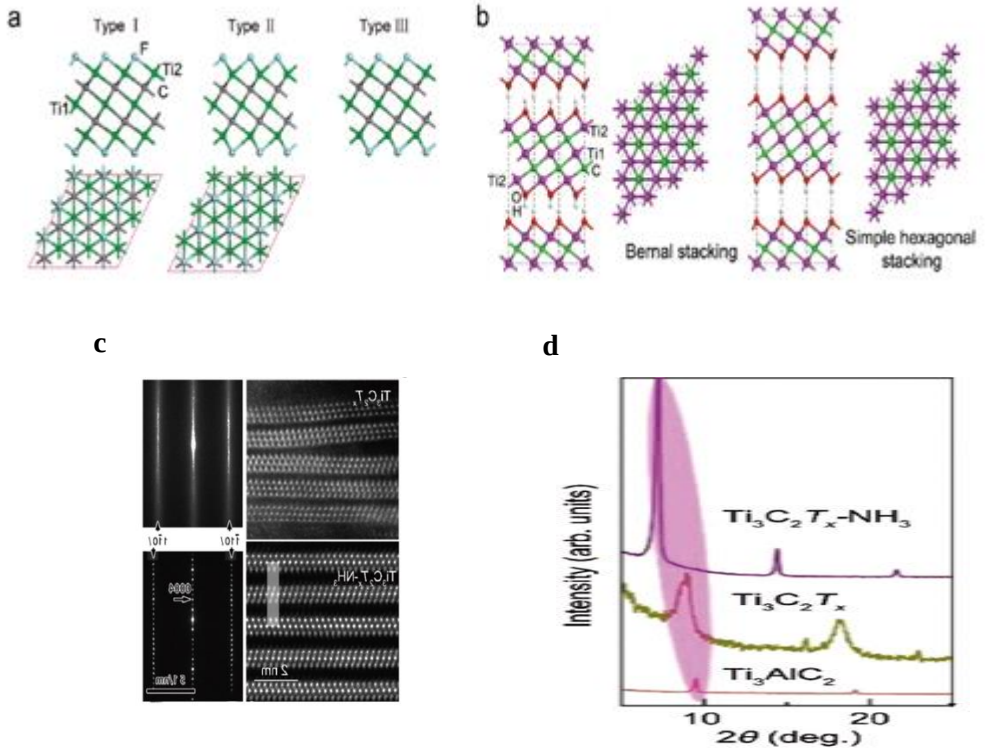

Fig 3 (a) Various structural configurations of $Ti_3C_2F_2$ are depicted in Fig. 3, showing different arrangements of surface F atoms from side and top views (source: American Chemical Society, copyright 2012, ref. [112]). (b) Fig. 3 also presents projections of two distinct stacking types of $Ti_3C_2(OH)_2$ (source: Nature, copyright 2015, ref. [113]). (c) The structure and diffraction patterns of $Ti_3C_2T_x$ and annealed $Ti_3C_2T_x$ in ammonia are captured through STEM imaging along the [11 %20] zone axis (source: American Chemical Society, copyright 2014, ref. [114]; copyright 2019, ref. [115]; and copyright 2019, ref. [116]). (d) X-ray diffraction (XRD) patterns of Ti_3AlC_2, $Ti_3C_2T_x$, and annealed $Ti_3C_2T_x$ in ammonia are displayed (source: American Chemical Society, copyright 2019, ref. [116]).

Characterization techniques like annular dark-field imaging in scanning transmission electron microscopy (STEM) enable the identification of MX layer structures, while other methods like Raman spectroscopy and NMR studies provide indirect information about the composition and distribution of functional groups. MXene layers can be identified through significant shifts in the (00l) reflections in XRD

patterns when wet MXene powders undergo drying [19]. However, MXenes without terminations, except for Mo_2C, WC, and TaC crystals synthesized through CVD, have not been successfully produced yet [20]. Moreover, the preparation of MXenes with a single surface group termination is extremely challenging, and there are limited reports on this subject matter.

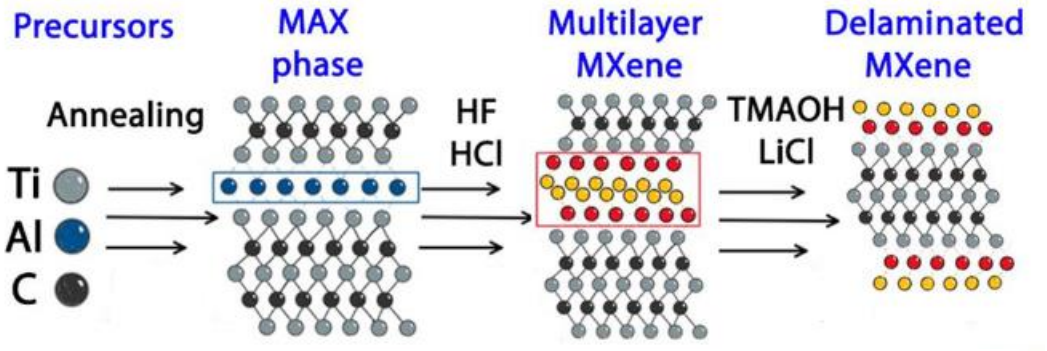

Fig 4. Showing the difference between MAX phase and MXene. Reproduced from permission from ref. [117], copyright 2021, ACS Chemical Health and Safety.

2.2.Electrical and optical properties: -

The investigation of MXenes' electronic properties is driven by their significant role in the performance of electrochemical capacitor devices. Bare MXenes, similar to their precursor MAX phases, exhibit metallic conductivity. However, when MXenes are terminated with surface functional groups, their conductivity can be altered. For example, Ti_2C in its bare form displays metallic features, but O-terminated MXenes like Ti_2CO_2 acquire semiconducting characteristics as the d band is lifted above the Fermi level. The type of termination also influences conductivity. MXenes functionalized with F, such as Ti_2CF_2, remain metallic with the Fermi energy located at the Ti layer's d band. Additionally, the electronic properties depend on the M element. Transitioning from $Ti_3C_2O_2$ to $Mo_2TiC_2O_2$ transforms metallic conductivity into a semiconducting nature [21]. Other MXenes like Hf_2CO_2, Zr_2CO_2, and Sc_2CT_2 (T = O, F, OH) are predicted to be semiconducting compounds. Certain MXenes, such as oxide $M'_2M''C_2$ (M' = Mo, W; M'' = Ti, Zr, Hf), are demonstrated to be topological insulators [22]. Defects in MXenes, like carbon vacancies in Ti_2CT_2, enhance their electronic conductivity [23].

In practice, MXenes prepared from MAX phases are typically terminated with mixed functional groups. Therefore, experimental assessments are necessary to evaluate the properties of prepared MXenes. Various MXene species, including Ti_2CT_x [24], $Ti_3C_2T_x$ [25], $TiNbCT_x$ [26], Ti_3CNT_x [26], $Ta_4C_3T_x$ [26], Mo_2CT_x [27], $Mo_2TiC_2T_x$ [28], and $Mo_2Ti_2C_3T_x$ [28], have been experimentally measured for their electronic properties. $Ti_3C_2T_x$, the first explored MXene, remains the most conductive with a linear I-V curve indicating its metallic nature [26]. This metallic $Ti_3C_2T_x$ exhibits potential as a supercapacitor electrode material. MXenes containing Mo exhibit semiconductor-like transport behavior, which is more suitable for applications like transistors. However, 2D $Mo_{4/3}C$ sheets with ordered metal divacancies possess high electrical conductivities, making them ideal for supercapacitor electrode materials [29]. The electrical conductivity of MXenes is also influenced by the sample state and preparation method. $Ti_3C_2T_x$ flakes, vacuum-filtered [30] or spin-cast [31] films, demonstrate high electrical conductivity. The conductivity of multilayered MXenes shows anisotropy, with lower conductivity along the c-axis compared to the basal plane [32]. Intercalation and surface termination have been experimentally shown to impact MXene electronic properties. Vacuum annealing leads to de-intercalation and partial surface functional group removal, significantly reducing the resistance of multilayered MXene [33]. Surface group tuning also modifies carrier transport properties.

Furthermore, thinner $Ti_3C_2T_x$ MXene films exhibit both transparency and conductivity, making them promising candidates for transparent conductive electrodes. For instance, a 5 nm-thick $Ti_3C_2T_x$ film transmits 91.2% of visible light with a resistance of 8 $k\Omega\ sq^{-1}$ [34], [35]. The optoelectronic behavior of these films can be tuned through cation intercalation. Therefore, when metallic MXenes are employed in supercapacitor applications, careful attention should be given to the sample state and preparation method.

2.3.Mechanical properties: -

The electrochemical performance of electrode materials can be influenced by their mechanical properties, especially in flexible applications where they undergo pressure, bending, and twisting. The mechanical characteristics of MXenes have been studied through theoretical calculations, considering factors such as thickness, surface terminations, and composition. The in-plane stiffness (C) and out-of-plane rigidity (D) of MXenes play a role in determining their elasticity and flexibility. The Foppl-von Karman numbers per area (C/D) of MXenes, which serve as flexibility descriptors, are comparable to those of the MoS_2 monolayer [36], indicating that MXenes are strong yet flexible materials. The in-plane Young's moduli of bare monolayer Ti_2C, Ti_3C_2, and Ti_4C_3 are 597 GPa, 502 GPa, and 534 GPa, respectively, making them weaker than atomically thin graphene but stronger than materials like MoS_2 and other 2D materials [37]. The calculated breaking strength of bare MXenes (M = Sc, Mo, Ti, Zr, Hf; X = C, N; n = 1) ranges from 92 to 161 N m^{-1} [38], indicating good mechanical stability. Surface termination in $Ti_{n+1}C_n$ (n = 1, 2, and/or 3) MXenes can slow down the collapse of surface atomic layers and enhance their mechanical flexibility [39], enabling them to sustain large strains under tensile loading.

Experimental investigations have also been conducted to examine the mechanical properties of MXenes. Nanoindentation experiments on individual layers of $Ti_3C_2T_x$ demonstrated Young's modulus of approximately 0.33 TPa [40], which is the highest among solution-processed 2D materials, including graphene oxide. $Ti_3C_2T_x$ films exhibit remarkable mechanical robustness and flexibility, as a 5 mm-thick film can withstand about 4000 times its weight (approximately 1.3 MPa) without visible deformation or damage and can be folded [41]. The mechanical properties of $Ti_3C_2T_x$ films can be further improved by compounding with polymers [41]or cellulose [42] nanofibrils. Additionally, during the electrochemical reaction process involving alkaline cation intercalation/extraction, the elastic modulus normal to the electrode surface undergoes reversible changes, ensuring structural stability during prolonged charge/discharge cycles [43].

2.4. Chemical stability: -

Based on Bader charge analysis, the oxidation number of M elements in MXenes is considerably lower than that of their corresponding oxides, which are the most thermodynamically stable species [44]. This indicates that MXenes have a tendency towards oxidation. Interestingly, the oxidation state of M in MXenes is strongly influenced by the functional terminations and can be adjusted through mild oxidation, where MXenes act as reductants and noble metal ions act as oxidants. Unlike complete oxidation into oxides, mild oxidation allows for the preservation of structural integrity while facilitating the formation of noble metal nanoparticles. Notably, these noble metal nanoparticles are uniformly distributed on MXenes, providing them with attractive surface-enhanced Raman scattering properties [45].

In the fabrication of films or coating electrodes, colloidal solutions of delaminated MXene flakes in water have been commonly used. Therefore, the stability of MXene suspensions is crucial for the investigation. $Ti_3C_2T_x$ MXene solutions in ambient environments degrade completely within 15 days, primarily forming anatase TiO_2 due to dissolved oxygen, the main oxidant for MXene flakes [46]. To prevent oxidation, sodium L-ascorbate can be added as an antioxidant to the colloidal $Ti_3C_2T_x$ MXene [47]. The quality guarantee period increases significantly when the $Ti_3C_2T_x$ MXene is dried, but the conductivity of MXene flakes still deteriorates over time due to edge oxidation. Furthermore, re-dispersing the dried sample in water becomes challenging. The degradation process also depends on the size of MXene, with smaller flakes being less stable and multilayered MXene exhibiting greater stability than monolayered MXene. Additionally, exposure to light accelerates the oxidation process [48]. To prolong storage time, MXene should be stored in a hermetically sealed container filled with argon at a temperature of 5°C in a dark environment.

Regarding thermal stability, dried MXenes exhibit different oxidation resistance behaviors depending on their composition and the surrounding environment. Multilayered Ti_2CT_x transforms into TiO_2 nanocrystals on thin graphitic nanosheets

at 227°C in air [49]. $Ti_3C_2T_x$ undergoes the partial transformation into TiO_2 (anatase) at 200°C and completely oxidizes into TiO_2 (rutile), releasing CO_2 and H_2Oat 1000°C in an oxygen atmosphere, although its stability cannot match that of graphite. In an argon atmosphere, $Ti_3C_2T_x$ remains stable up to temperatures of 800°C [50]. In the case of Nb_2CT_x, the surfaces are strongly decorated with Nb adatoms that attract and bond with ambient oxygen species, forming clusters that grow over time. V_2CT_x MXene remains stable in an argon atmosphere at temperatures below 375°C but begins to degrade at 150°C in an air atmosphere [51], [52].

3. SYNTHESIS OF $Ti_3C_2T_X$ MXENE

The exceptional parcels of $Ti_3C_2T_x$ are nearly related to its conflation processes, which determine its chemical composition, electrical conductivity, side size, etching effectiveness, face terminations, and blights. Since the original conflation of $Ti_3C_2T_x$ in 2011, experimenters have conducted expansive examinations into the new MAX phase and the drawing system. Presently, colorful types of etchants are being explored for the product of $Ti_3C_2T_x$ MXene, including fluoride drawing, fluoride-grounded swab drawing, and fluoride-free drawing. These different drawing approaches have a substantial influence on the electrochemical performance of $Ti_3C_2T_x$ MXene.

3.1.HF Etching: -

MXene is typically prepared by selectively etching the A layer of the MAX phase, and the mechanism can be described as follows [53], [54]:

$$M_{(n+1)}AX_n + 3HF = AlF_3 + 1.5H_2 + M_{(n+1)}X_n \text{……(1)}$$

$$M_{(n+1)}X_n + 2H_2O = M_{(n+1)}X_n(OH)_2 + H_2 \text{……....(2)}$$

$$M_{(n+1)}X_n + 2HF = M_{(n+1)}X_nF_2 + H_2 \text{…….……(3)}$$

In reaction (1), the separation of the A elements from the MAX phase leads to the formation of the $M_{n+1}X_n$ phase. The functional groups such as -F and/or -OH originate from reactions (2) and (3). Figure 5 depicts the exfoliation process and the characterization of the structural morphology of Ti_3AlC_2. Naguib et al. achieved the

synthesis of $Ti_3C_2T_x$ MXene with an accordion-like shape by etching Ti_3AlC_2 powders for 2 hours in a 50% concentrated HF solution [55]. Mashtalir et al. [56] examined the effects of process parameters and particle size on the etching process of Al from Ti_3AlC_2 using a 50% HF solution. The findings indicated that reducing the initial particle size of MAX, prolonging the reaction time, and increasing the immersion temperature favored the transformation of bulky Ti_3AlC_2 into $Ti_3C_2T_x$ [57]. The etching procedure is significantly influenced by the duration of etching, temperature, and HF concentration. Al can be effectively removed from the Ti_3AlC_2 MAX phase using HF concentrations as high as 5%. Still, an accordion- such like flyspeck form is generally observed when HF attention exceeds 10%. Additionally, the increase in HF concentration leads to a higher presence of defects in the $Ti_3C_2T_x$ flakes, impacting the quality, stability in the environment, and properties of the resulting MXene [58], [59]. Although the HF method has the advantages of low reaction temperature and ease of operation, it should be noted that HF etchant is highly corrosive, toxic, poses operational risks, and has adverse environmental effects.

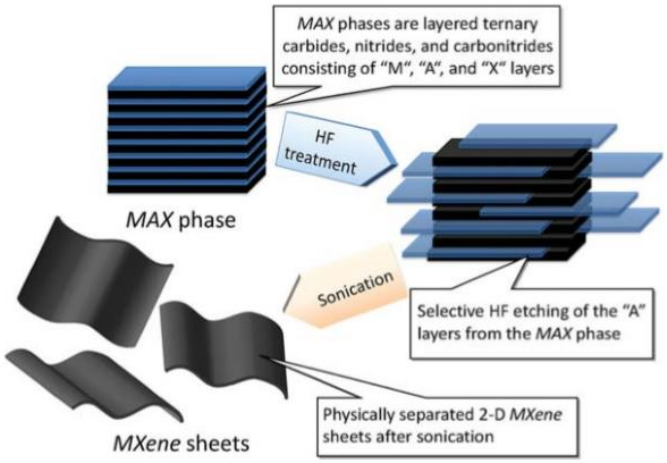

Fig 5. Illustration of schematics depicting the synthesis process of MXene using HF as the etchant to obtain single-layered MXene configuration from the MAX phase. Reproduced with permission from ref. [118], copyright 2012, America Chemical Society.

3.2. Acid/fluoride salt or Hydrofluoride Etching: -

Apart from HF etching, alternative milder etchants containing fluorine, such as $(NH_4)HF_2$, HCl/NH_4F, HCl/NaF, HCl/KF, HCl/FeF_3, and HCl/LiF, have been developed for in situ production of HF for etching. It is important to note that these etchants are specifically applicable to the preparation of $Ti_3C_2T_x$ MXene and may not be suitable for other MXenes. For example, only the NaF/HCl etchant is effective for producing highly pure V_2C MXene [60], although it requires longer etching time compared to pure HF etching, it enhances the safety of the experimental process. The MXene obtained using these etchants still exhibits an accordion-like multilayered morphology [60]. During the etching process, cations such as $NH4^+$, Na^+, K^+, and Fe^{3+} are simultaneously intercalated into the MXene interlayers. This cation intercalation results in a more open and uniform structure of MXene layers compared to the pristine MXene, with atomic layers being more evenly spaced. In the case of etching Ti_3AlC_2 using HCl/FeF_3, Fe^{3+} cations partially oxidize the surface Ti due to the extraction of Al [61].

Among the etchants discussed, HCl/LiF has been predominantly used and proven to be the most effective. By selecting the appropriate concentration (7.5 M LiF in 9 M HCl), delamination is achieved through the intercalation of solvated Li+ ions. Consequently, larger single- or few-layer MXene flakes with fewer defects can be readily obtained by hand-shaking without the need for sonication or further intercalation [62]. The choice of precursor MAX phases determines the grain sizes and shapes of the resulting MXenes, allowing researchers to select appropriate MAX phases based on specific research objectives. Notably, the MXene sediment obtained exhibits clay-like behavior due to the intercalation of Li^+ ions, leading to changes in rheological properties [63]. This offers new processing options such as direct film production through rolling. Additionally, the MXene sediment demonstrates superior hydrophilicity attributed to surface O-containing groups and a high negative surface charge, as confirmed by potential measurements (-30 to -80 mV) [64]. As a result, the MXene can be easily dispersed in water and processed using techniques like spin coating [64], spray coating [65], printing [66], and writing [67].

Compared to pure HF etching, the LiF/HCl etching method provides several advantages, although it requires a longer etching time. NMR characterization reveals that the synthesis method influences the surface termination of the MXene. HF-etched MXene has nearly four times more -F termination compared to LiF/HCl-etched MXene. However, -F groups are known to have a negative impact on the electrochemical performance of MXene, which explains why HF-etched MXene exhibits lower capacitance. Interestingly, MXene epitaxial thin films can be directly obtained from sputtering-deposited MAX thin films through acid etching.

HCl/LiF has proven to be an effective etchant for MXene synthesis, offering both exfoliation and delamination effects. However, it remains a puzzle as to why only HCl/LiF etchant exhibits these properties. Preliminary research by Lerf et al. 1977[68]suggests that the presence of anions larger than F^- or O^{2-} during etching, such as Cl^-, Br^-, I^-, SO_4^{2-}, and PO_4^{3-}, results in more open MXene interlayers. It is hypothesized that these anions adsorb at the edges of MXenes, acting as props to open the edges and allowing easier access for water into the interlayer. Among these anions, Cl^- is readily adsorbed onto MXene edges and demonstrates a significant synergistic effect on swelling, which is why an HCl solution is preferred during etching [69].

Regarding cations, Li^+ ions, accompanied by water molecules, can enter the interlayer space, causing swelling and delamination [69]. Exploring the effects of various ions during etching is crucial to develop more effective and rational methods for MXene preparation.

3.3. Alkali Etching: -

To our current understanding, the presence of protons and fluoride ions is essential for the preparation of MXene through acidic solution etching. However, considering the hazards associated with hydrofluoric acid (HF) and the negative impact of -F groups on MXene's electrochemical performance, there is a pressing need for

alternative fluorine-free methods. Significant efforts have been dedicated to developing fluorine-free alkali-etching methods.

One approach involves using tetramethylammonium hydroxide (TMAOH) to remove the Al layer from Ti_3AlC_2 after pretreating the Ti_3AlC_2 surface with 20-30 wt% HF for a short period [70]. However, it has been observed that using only TMAOH as the etchant is unable to reproduce the desired results, indicating that both HF and TMAOH contribute to the etching process. Another strategy, proposed for the synthesis of smaller MXene structures like quantum dots, involves TBAOH (tetra-n-butylammonium hydroxide) intercalation with sonication [71].

In addition to organic alkalies, inorganic alkalies have also been frequently employed in Ti_3AlC_2 etching. An inorganic alkali-assisted hydrothermal method has been utilized to prepare MXenes. $Ti_3C_2T_x$ powder has been successfully synthesized in KOH solution with a small amount of water at a temperature of 180°C or in a NaOH aqueous solution at an elevated temperature of 270°C. This inorganic alkali-based method has yielded multilayer $Ti_3C_2T_x$ with -OH and -O terminations and a purity of 92 wt% [72].

4. MXENE APPLICATIONS

MXenes, a groundbreaking class of two-dimensional nanosheets, have opened up a world of possibilities in various applications. With their remarkable conductivity and customizable properties, these materials are at the forefront of revolutionizing technologies such as supercapacitors with rapid charging capabilities and developing advanced drug delivery systems with unique properties to precisely target and release therapeutic agents, leading to more effective treatments with reduced side effects. Below are listed some of the applications of MXene in various fields.

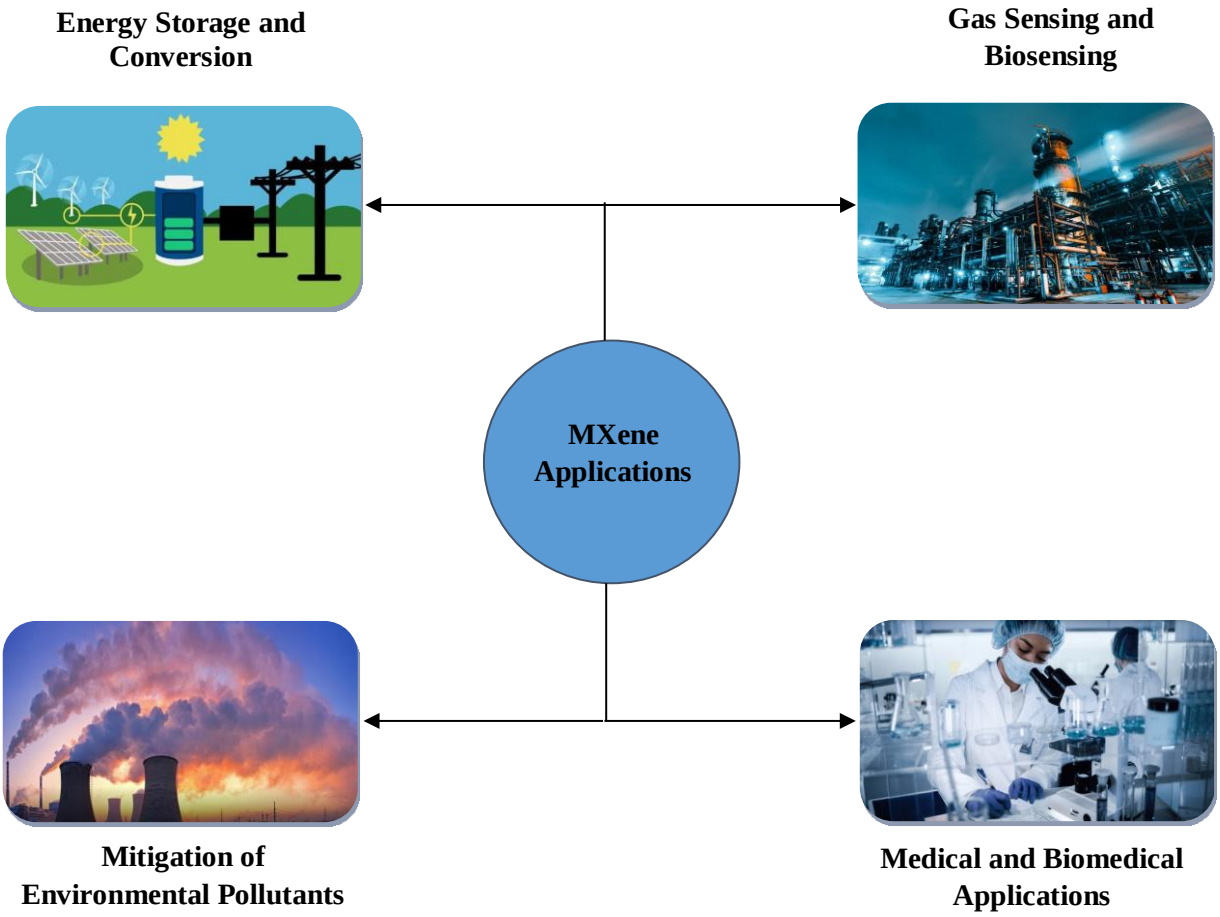

Fig 3. Showing applications of MXene in different fields.

4.1. Energy Storage and Conversion: -

MXenes are highly versatile materials with a wide range of applications due to their attractive properties, including high Young's modulus, excellent electrical conductivity, and customizable surface chemistry. These attributes make them appealing for use in catalytic processes and energy storage applications [73]. MXenes find practical use in energy storage technologies such as fuel cells, hydrogen storage, lithium-ion batteries, and supercapacitors [74]– [77]. Additionally, they demonstrate promising results in fields like optoelectronics, flexible electronics, wearable devices, and various environmental and biomedical applications.

Because of the depletion of fossil fuels and the growing energy demands, there is a heightened interest in renewable energy sources and energy conversion systems [78]. Lithium-ion batteries and supercapacitors, in particular, are gaining attention due to their superior power densities and specific capacitance, making them suitable for compact and integrated applications, like mobile phones, tablets, automotive systems, and other power sources. MXenes offer a compelling material choice for supercapacitors, which serve as a potential alternative for energy storage due to their cyclic stability and improved charge/discharge rates compared to traditional batteries.

For instance, multilayered $Ti_3C_2T_x$, studied as a supercapacitor material, exhibits a specific capacitance of 340 F cm^{-2} in a basic KOH electrolytic solution [79]. Furthermore, $Ti_3C_2T_x$ thin-film electrodes in a 1M Na_2SO_4 solution showcase a volumetric capacitance of 900 F cm^{-3} at a scan rate of 20 mV/s, displaying excellent cycle stability even after 10,000 cycles [80]. These findings highlight the promising potential of MXenes in advancing energy storage and conversion technologies.

MXenes exhibit distinct charge/discharge mechanisms in different electrolytes, leading to varied behavior. In acidic electrolytes, $Ti_3C_2T_x$ mainly functions as a pseudocapacitor, while in neutral or alkaline electrolytes, it behaves as a double-layer capacitor, although with reduced performance. The pseudocapacitance arises primarily due to reversible redox reactions occurring near the electrode surface. This results in MXene-based pseudocapacitors having high energy density, while double-layer capacitance relies on reversible electrolyte ion accumulation without redox reactions (physical adsorption mechanism). MXenes demonstrate superior electrochemical performance in acidic electrolytes compared to aqueous or alkaline electrolytes.

The surface chemistry of MXenes significantly influences their supercapacitor properties, as surface metrics directly impact the volumetric capacitance. Surface termination with F or O functional groups enhances specific capacitance. Chemical modifications during MXene synthesis using NH_4, DMSO, KOH, or heat treatment substantially increase specific capacitance, particularly in acidic electrolytes. MXenes

like Mo_2CT_x and $Mo_{1.33}CT_x$ have also shown promising supercapacitor performance, with $Mo_{1.33}CT_x$ exhibiting a 65% higher specific capacitance than Mo_2CT_x, attributed to the beneficial effect of vacancies. The flake size of MXenes has been linked to specific capacitance, although experimental validation is still needed [81].

MXenes tend to accumulate through hydrogen bonding and van der Waals forces, resulting in limited ion exchange and accessibility due to reduced surface area. However, these limitations can be addressed using macroporous structures, hydrogels, aligned crystalline structures, and new architectural designs. For example, $Ti_3C_2T_x$-polypyrrole nanocomposite and $(Mo_{2/3}Y_{1/3})CTx$ and $Ti_3C_2T_x$ hydrogels have been reported, exhibiting specific capacitance values of 1000 F cm^{-2} and above [82].

Regarding Li-ion batteries, which are widely used in portable electronic devices for power and energy storage, MXenes hold promise as electrode materials. They offer higher electronic conductivity and a specific surface area that enables efficient Li storage at lower circuit voltages compared to conventional materials like graphite [83]. MXenes such as $Ti_3C_2T_x$ thin film have demonstrated gravimetric capacity over 410 mg/g, similar to Mo_2CT_x (423 mg/g) [84]. Known MXenes for Li-ion storage include Nb_2CT_x and V_2CT_x, with some other options predicted theoretically, such as Cr^-, Zr^-, and Mn^-based MXenes [84], [85].

Although there has been extensive research on $Ti_3C_2T_x$, theoretical observations suggest that MXenes with lower stoichiometric indexes (M_4X_3, M_3X_3, and M_2X) exhibit increased gravimetric capacities[86]. For instance, Ti_2C demonstrated a 50% higher Li^+ gravimetric capacity compared to Ti_3C_2 [87]. Monolayered MXenes generally exhibit higher gravimetric capacities than multilayers due to maximum Li adsorption during intercalation.

The presence of functional groups in MXenes has significant effects on metallic ion adsorption, storage capacity, intercalation, and operating potential. Particularly, the presence of F and OH terminal groups improves the diffusion barrier. For example, the

Li-ion capacity of $Ti_3C_2T_x$ increases nearly fivefold in the presence of OH termination [88]. Theoretical studies also indicate an increase in storage capacity with O termination [89]. O-terminated pristine M_2C compounds with light transition metals are considered the most promising MXene anode materials for Li-ion batteries. To enhance MXene capacity, the HCl - LiF synthesis route is preferred over HF methods. HCl - LiF synthesis leads to fewer F and OH terminations, reduced structural defects, and improved delamination ratio, resulting in enhanced electrochemical performance [90]. Hence, a synthesis route that allows better control over surface chemistry significantly contributes to improving MXene's electrochemical performance.

4.2. Gas sensing and Biosensing: -

Sensing tools play a crucial role in monitoring substance concentrations for the sake of human and environmental safety in various applications. The success criteria for sensing devices include a low detection limit, high sensitivity, short response time, wide linear range, and excellent selectivity for specific analytes. Additionally, cost-effectiveness is essential to facilitate easy commercialization. MXenes exhibit intriguing properties that make them suitable for sensing device applications. For instance, MXene-derived quantum dots have been shown to selectively quench the luminescence of Zn ions in the presence of various metal ions, making them promising for the fabrication of Zn^{2+} sensors [91].

In gas sensing applications, selective absorption and reversible release and capture of gases are critical. Ti_2C nanolayers have demonstrated excellent sensing ability for NH_3 due to the strategic positioning of N atoms above the Ti atoms in Ti_2CO_2nanolayers, resulting in stronger bonding through higher binding energy compared to other gases like H_2, CH_4, CO, CO_2, N_2, and NO_2 [92]. MXene monolayers can efficiently release NH_3 upon reduction of biaxial strains, and after adsorption, MXenes exhibit increased electrical conductivity [93]. O-terminated MXenes offer reversible NH_3 adsorption, and M_2CO_2 MXenes (where M represents Sc, Ti, Zr, and Hf) have been studied for gas-sensing applications [94]. The mechanism of NH_3 adsorption involves chemical-

adsorption on M_2CO_2 with charge transfer, leading to control over NH_3 adsorption [93]. An increase in adsorption energy enables a shift from chemisorption to physisorption, resulting in the reversible behavior of NH_3 adsorption. Therefore, O-terminated MXenes show promise as candidates for gas sensing and capturing applications.

MXene-based composites have demonstrated promising capabilities in detecting macromolecules, cells, gases, and small molecules. For instance, Ti_3C_2 quantum dots synthesized using a simple hydrothermal method at varying temperatures (100°C, 120°C, and 150°C) exhibited photoluminescence with quantum yields of approximately 10% [95]. These quantum dots were utilized for cellular probing invitro bioimaging of RAW 264.7 cells [96]. Additionally, MXenes have been effectively employed for detecting neural activity by incorporating them into ultrathin conductive films along with field-effect transistors [97]. This setup enabled the detection of the neurotransmitter dopamine through π-π interactions between dopamine molecules and electrons from MXene termination groups (O, H, or F). The sensing device also allowed real-time monitoring of cultured primary hippocampus neurons, showing excellent biocompatibility during long-term culture.

MXenes, in general, exhibit tremendous potential for developing sensing devices catering to a wide range of applications, including environmental monitoring and biomedical detection. This is due to their outstanding conductivity, hydrophilicity, and biocompatibility, which make them highly versatile and suitable for various sensing applications.

4.3. Remediation of Environmental Pollutants: -

MXenes have been extensively investigated for their potential in absorbing various harmful pollutants, including uranyl, ammonia, lead (II), chromium (VI), copper, mercury, methylene blue, methane, and phosphate. Ti_3C_2 and $Ti_3C_2T_x$ are among the MXenes commonly used for environmental remediation. $Ti_3C_2(OH/ONa)_xF_{2-x}$ MXene

[98], synthesized through chemical exfoliation followed by alkalization intercalation, has been found to absorb more Pb(II) than other divalent ions such as Ca(II) and Mg(II) in a water-based solution. This behavior is attributed to the higher affinity of Ti_2O bond in the MXenes towards Pb (II), promoting the formation of inner-space complexes.

The redox properties of 2D $Ti_3C_2T_x$ have been utilized for the effective removal of toxic water pollutants, such as Cr(VI) [99]. The MXene facilitates a one-step procedure to reduce highly toxic Cr (VI) to less toxic Cr(III), making water safe for drinking. Additionally, $Ti_3C_2T_x$ mixed with $KMnO_4$ has been demonstrated to aid in the removal of Cu from water, outperforming commercially available activated carbon [100].

$Ti_3C_2OH_{0.8}F_{1.2}/Fe_2O_3$ nanocomposite has shown promise for phosphate removal through adsorption [101]. The integration of MXene with Fe_2O_3 increases the sorption capability due to Fe_3O_4 distribution on the MXene surface, enabling magnetic separation and enhancing the adsorption tendency.

MXenes also exhibit excellent sorption capability for removing dyes and harmful industrial wastes from water, particularly $Ti_3C_2T_x$, which can absorb and decompose organic compounds in aqueous media under UV irradiation [102]. The negatively charged surface of MXenes facilitates electrostatic interactions, leading to the efficient removal of methylene blue. Under UV light, MXenes show outstanding adsorbent capacity for water purification, removing both methylene blue and AB80 dyes from water solutions [103].

Overall, MXenes hold great potential as effective tools for environmental remediation, providing solutions for water purification and pollutant removal in various applications.

4.4. Medical and Biomedical Applications: -

The unique properties of MXenes make them suitable for anticancer therapies and bioimaging applications. Conventional cancer treatments like radiotherapy and

chemotherapy often have drawbacks, such as non-specificity and undesirable side effects. Hence, there is a need for more effective and compatible treatment methods. Photothermal therapy, a light-controlled approach, has shown promise in enhancing selectivity by using photothermal agents that convert laser energy into heat to target and destroy tumor cells [104].

Several nanomaterials, including Au nanorods, black phosphorus, carbon-based nanomaterials, and copper sulfide nanoparticles, have been explored for photothermal therapy. MXenes, particularly $Ti_3C_2T_x$ with near-infrared (NIR) absorption capabilities following Al-oxyanion termination, have also emerged as potential photothermal therapy agents [105]. In particular, $Ti_3C_2T_x$ sheets with OH or F termination have demonstrated promising results as photothermal agents against murine breast cancer.

MnO_x/Ti_3C_2 composite has been proposed for photothermal therapies and bioimaging [106]. Surface modification of the composite with soybean phospholipids resulted in effective cancer cell killing and tumor growth suppression after infrared laser irradiation [107].

MXene quantum dots prepared using a safe and fluorine-free method have shown high photothermal conversion efficiency, making them effective in killing cervical cancer cells in vivo and in vitro after intravenous injection into mice at low concentrations [108].

Researchers have integrated Ti_3C_2 MXene with 3D-printed bioactive glass scaffolds to fabricate Ti_3C_2-BG scaffolds [109]. These scaffolds exhibited high photothermal conversion efficiency, leading to complete tumor eradication through photothermal hyperthermia and the accelerated growth of newly born bone tissue in vivo. The dual functionality of these composite scaffolds makes them highly attractive for bone tumor treatment.

In summary, MXenes offer promising prospects for enhancing cancer therapies through photothermal therapy, and their unique properties make them versatile candidates for both cancer treatment and bioimaging applications.

5. OVERCOMING OBSTACLES AND EMBRACING POSSIBILITIES

MXenes, a novel class of 2D materials with unique properties, hold immense potential for various applications. Despite their exceptional mechanical, electronic, optical, and magnetic characteristics, most of the research has been theoretical, lacking experimental validation. However, the focus has shifted towards exploring specific applications. The synthesis and surface termination techniques significantly impact the MXene properties, and delamination processes with appropriate surface terminations have shown promising results for energy storage, catalysis, and EMI shielding applications. Further research is needed to optimize MXene surface functionalization for improved chemical applicability.

Combining experimental and theoretical approaches will be essential to uncover MXenes' complex properties and meet future demands. Continuity in research is crucial, especially regarding the discovery of missing MAX phases like Ti_3AlN_2 and Ti_2SiC, as well as exploring novel MXenes with thermodynamically stable stoichiometries and investigating superconductivity and novel magnetic phases. Efforts to narrow the theoretical and experimental gap and explore the effect of doping on MAX phases for tunable conductivity should be intensified. Understanding the anisotropy in electronic properties through momentum dependence measurements will further enhance our comprehension of MAX phases.

Furthermore, developing modern synthesis and material processing techniques for corrosion- and oxidation-resistant MAX phases with low friction, retaining exceptional strength, will be instrumental in advancing MXene applications.

In conclusion, a multidisciplinary approach involving both theoretical and experimental methods is crucial for unlocking the full potential of MXenes and discovering new possibilities for their application in various technological challenges.

REFERENCES: -

[1] C. Tan *et al.*, "Recent Advances in Ultrathin Two-Dimensional Nanomaterials," *Chem Rev*, vol. 117, no. 9, pp. 6225–6331, May 2017, doi: 10.1021/ACS.CHEMREV.6B00558.

[2] V. Nicolosi, M. Chhowalla, M. G. Kanatzidis, M. S. Strano, and J. N. Coleman, "Liquid Exfoliation of Layered Materials," *Science (1979)*, vol. 340, no. 6139, 2013, doi: 10.1126/SCIENCE.1226419.

[3] K. S. Novoselov*et al.*, "Two-dimensional atomic crystals," *Proc Natl Acad Sci U S A*, vol. 102, no. 30, pp. 10451–10453, Jul. 2005, doi: 10.1073/PNAS.0502848102.

[4] M. Naguib *et al.*, "Two-Dimensional Nanocrystals Produced by Exfoliation of Ti3AlC2," *Advanced Materials*, vol. 23, no. 37, pp. 4248–4253, Oct. 2011, doi: 10.1002/ADMA.201102306.

[5] K. Nabeela and N. B. Sumina, *MXenes and their composites as piezoresistive sensors*. Elsevier, 2021. doi: 10.1016/B978-0-12-823361-0.00011-3.

[6] R. M. Ronchi, J. T. Arantes, and S. F. Santos, "Synthesis, structure, properties and applications of MXenes: Current status and perspectives," *Ceram Int*, vol. 45, no. 15, pp. 18167–18188, Oct. 2019, doi: 10.1016/J.CERAMINT.2019.06.114.

[7] M. W. Barsoum, "The MN+1AXN phases: A new class of solids: Thermodynamically stable nanolaminates," *Progress in Solid State Chemistry*, vol. 28, no. 1–4, pp. 201–281, Jan. 2000, doi: 10.1016/S0079-6786(00)00006-6.

[8] B. Anasori, M. R. Lukatskaya, and Y. Gogotsi, "2D metal carbides and nitrides (MXenes) for energy storage," *Nat Rev Mater*, vol. 2, no. 2, Jan. 2017, doi: 10.1038/NATREVMATS.2016.98.

[9] P. O. Å. Persson and J. Rosen, "Current state of the art on tailoring the MXene composition, structure, and surface chemistry," *CurrOpin Solid State Mater Sci*, vol. 23, no. 6, Dec. 2019, doi: 10.1016/J.COSSMS.2019.100774.

[10] M. Naguib, V. N. Mochalin, M. W. Barsoum, and Y. Gogotsi, "25th anniversary article: MXenes: a new family of two-dimensional materials," *Adv Mater*, vol. 26, no. 7, pp. 992–1005, Feb. 2014, doi: 10.1002/ADMA.201304138.

[11] J. Zhu *et al.*, "Recent advance in MXenes: A promising 2D material for catalysis, sensor and chemical adsorption," *Coord Chem Rev*, vol. 352, pp. 306–327, Dec. 2017, doi: 10.1016/J.CCR.2017.09.012.

[12] B. Zhou *et al.*, "Flexible, Robust, and Multifunctional Electromagnetic Interference Shielding Film with Alternating Cellulose Nanofiber and MXene Layers," *ACS Appl Mater Interfaces*, vol. 12, no. 4, pp. 4895–4905, Jan. 2020, doi: 10.1021/ACSAMI.9B19768/SUPPL_FILE/AM9B19768_SI_001.PDF.

[13] P. Eklund, J. Rosen, and P. O. Å. Persson, "Layered ternary Mn+1AXn phases and their 2D derivative MXene: An overview from a thin-film perspective," *J Phys D Appl Phys*, vol. 50, no. 11, Feb. 2017, doi: 10.1088/1361-6463/AA57BC.

[14] M. Khazaei*et al.*, "Novel Electronic and Magnetic Properties of Two-Dimensional Transition Metal Carbides and Nitrides," *Adv Funct Mater*, vol. 23, no. 17, pp. 2185–2192, May 2013, doi: 10.1002/ADFM.201202502.

[15] T. Hu, J. Wang, H. Zhang, Z. Li, M. Hu, and X. Wang, "Vibrational properties of Ti_3C_2 and $Ti_3C_2T_2$ (T = O, F, OH) monosheets by first-principles calculations: a comparative study," *Physical Chemistry Chemical Physics*, vol. 17, no. 15, pp. 9997–10003, Apr. 2015, doi: 10.1039/C4CP05666C.

[16] J. L. Hart *et al.*, "Control of MXenes' electronic properties through termination and intercalation," *Nat Commun*, vol. 10, no. 1, Dec. 2019, doi: 10.1038/S41467-018-08169-8.

[17] J. Halim *et al.*, "Transparent Conductive Two-Dimensional Titanium Carbide Epitaxial Thin Films," *Chem Mater*, vol. 26, no. 7, pp. 2374–2381, Apr. 2014, doi: 10.1021/CM500641A.

[18] X. Sang *et al.*, "Atomic Defects in Monolayer Titanium Carbide ($Ti_3C_2T_x$) MXene," *ACS Nano*, vol. 10, no. 10, pp. 9193–9200, Oct. 2016, doi: 10.1021/ACSNANO.6B05240.

[19] M. Alhabeb*et al.*, "Guidelines for Synthesis and Processing of Two-Dimensional Titanium Carbide ($Ti_3C_2T_x$MXene)," *Chemistry of Materials*, vol. 29, no. 18, pp. 7633–7644, Sep. 2017, doi: 10.1021/ACS.CHEMMATER.7B02847.

[20] Y. Gogotsi, "Chemical vapour deposition: Transition metal carbides go 2D," *Nat Mater*, vol. 14, no. 11, pp. 1079–1080, Nov. 2015, doi: 10.1038/NMAT4386.

[21] L. Li, "Lattice dynamics and electronic structures of $Ti_3C_2O_2$ and $Mo_2TiC_2O_2$ (MXenes): The effect of Mo substitution," *Comput Mater Sci*, vol. 124, pp. 8–14, Nov. 2016, doi: 10.1016/J.COMMATSCI.2016.07.008.

[22] M. Khazaei*et al.*, "Nearly free electron states in MXenes," *Phys Rev B*, vol. 93, no. 20, p. 205125, May 2016, doi: 10.1103/PHYSREVB.93.205125/FIGURES/6/MEDIUM.

[23] T. Hu, J. Yang, and X. Wang, "Carbon vacancies in Ti2CT2 MXenes: defects or a new opportunity?," *Physical Chemistry Chemical Physics*, vol. 19, no. 47, pp. 31773–31780, Dec. 2017, doi: 10.1039/C7CP06593K.

[24] J. Xu *et al.*, "MXene Electrode for the Integration of WSe_2 and MoS_2 Field Effect Transistors," *Adv Funct Mater*, vol. 26, no. 29, pp. 5328–5334, Aug. 2016, doi: 10.1002/ADFM.201600771.

[25] J. Halim *et al.*, "Transparent Conductive Two-Dimensional Titanium Carbide Epitaxial Thin Films," *Chem Mater*, vol. 26, no. 7, pp. 2374–2381, Apr. 2014, doi: 10.1021/CM500641A.

[26] M. Naguib *et al.*, "Two-dimensional transition metal carbides," *ACS Nano*, vol. 6, no. 2, pp. 1322–1331, Feb. 2012, doi: 10.1021/NN204153H.

[27] J. Halim *et al.*, "Transparent Conductive Two-Dimensional Titanium Carbide Epitaxial Thin Films," *Chem Mater*, vol. 26, no. 7, pp. 2374–2381, Apr. 2014, doi: 10.1021/CM500641A.

[28] B. Anasori*et al.*, "Control of electronic properties of 2D carbides (MXenes) by manipulating their transition metal layers," *Nanoscale Horiz*, vol. 1, no. 3, pp. 227–234, Apr. 2016, doi: 10.1039/C5NH00125K.

[29] Q. Tao *et al.*, "Two-dimensional $Mo_{1.33}C$ MXene with divacancy ordering prepared from parent 3D laminate with in-plane chemical ordering," *Nat Commun*, vol. 8, 2017, doi: 10.1038/NCOMMS14949.

[30] A. D. Dillon *et al.*, "Highly Conductive Optical Quality Solution-Processed Films of 2D Titanium Carbide," *Adv Funct Mater*, vol. 26, no. 23, pp. 4162–4168, Jun. 2016, doi: 10.1002/ADFM.201600357.

[31] F. Shahzad *et al.*, "Electromagnetic interference shielding with 2D transition metal carbides (MXenes)," *Science*, vol. 353, no. 6304, pp. 1137–1140, Sep. 2016, doi: 10.1126/SCIENCE.AAG2421.

[32] T. Hu, J. Wang, H. Zhang, Z. Li, M. Hu, and X. Wang, "Vibrational properties of Ti_3C_2 and $Ti_3C_2T_2$ (T = O, F, OH) monosheets by first-principles calculations: a comparative study," *Physical Chemistry Chemical Physics*, vol. 17, no. 15, pp. 9997–10003, Apr. 2015, doi: 10.1039/C4CP05666C.

[33] J. L. Hart *et al.*, "Control of MXenes' electronic properties through termination and intercalation," *Nat Commun*, vol. 10, no. 1, Dec. 2019, doi: 10.1038/S41467-018-08169-8.

[34] J. Halim *et al.*, "Transparent Conductive Two-Dimensional Titanium Carbide Epitaxial Thin Films," *Chem Mater*, vol. 26, no. 7, pp. 2374–2381, Apr. 2014, doi: 10.1021/CM500641A.

[35] A. D. Dillon *et al.*, "Highly Conductive Optical Quality Solution-Processed Films of 2D Titanium Carbide," *Adv Funct Mater*, vol. 26, no. 23, pp. 4162–4168, Jun. 2016, doi: 10.1002/ADFM.201600357.

[36] T. Hu, J. Yang, and X. Wang, "Carbon vacancies in Ti_2CT_2MXenes: defects or a new opportunity?," *Physical Chemistry Chemical Physics*, vol. 19, no. 47, pp. 31773–31780, Dec. 2017, doi: 10.1039/C7CP06593K.

[37] S. Huang, K. C. Mutyala, A. V. Sumant, and V. N. Mochalin, "Achieving superlubricity with 2D transition metal carbides (MXenes) and MXene/graphene coatings," *Mater Today Adv*, vol. 9, p. 100133, Mar. 2021, doi: 10.1016/J.MTADV.2021.100133.

[38] B. Yorulmaz, A. Özden, H. Şar, F. Ay, C. Sevik, and N. K. Perkgöz, "CVD growth of monolayer WS_2 through controlled seed formation and vapor density," *Mater Sci Semicond Process*, vol. 93, pp. 158–163, Apr. 2019, doi: 10.1016/J.MSSP.2018.12.035.

[39] Z. Guo, J. Zhou, C. Si, and Z. Sun, "Flexible two-dimensional $Ti_{n+1}C_n$ (n = 1, 2 and 3) and their functionalized MXenes predicted by density functional theories," *Physical Chemistry Chemical Physics*, vol. 17, no. 23, pp. 15348–15354, Jun. 2015, doi: 10.1039/C5CP00775E.

[40] A. Lipatov*et al.*, "Elastic properties of 2D $Ti_3C_2T_x$MXene monolayers and bilayers," *Sci Adv*, vol. 4, no. 6, Jun. 2018, doi: 10.1126/SCIADV.AAT0491.

[41] Z. Ling *et al.*, "Flexible and conductive MXene films and nanocomposites with high capacitance," *Proc Natl Acad Sci U S A*, vol. 111, no. 47, pp. 16676–16681, Nov. 2014, doi: 10.1073/PNAS.1414215111.

[42] W. Tian *et al.*, "Multifunctional Nanocomposites with High Strength and Capacitance Using 2D MXene and 1D Nanocellulose," *Adv Mater*, vol. 31, no. 41, Oct. 2019, doi: 10.1002/ADMA.201902977.

[43] J. Come *et al.*, "Nanoscale Elastic Changes in 2D $Ti_3C_2T_x$ (MXene) Pseudocapacitive Electrodes," *Adv Energy Mater*, vol. 6, no. 9, May 2016, doi: 10.1002/AENM.201502290.

[44] T. Hu, J. Yang, W. Li, X. Wang, and C. M. Li, "Quantifying the rigidity of 2D carbides (MXenes)," *Physical Chemistry Chemical Physics*, vol. 22, no. 4, pp. 2115–2121, Jan. 2020, doi: 10.1039/C9CP05412J.

[45] K. Li *et al.*, "An Ultrafast Conducting Polymer@MXene Positive Electrode with High Volumetric Capacitance for Advanced Asymmetric Supercapacitors," *Small*, vol. 16, no. 4, p. 1906851, Jan. 2020, doi: 10.1002/SMLL.201906851.

[46] C. J. Zhang *et al.*, "Oxidation Stability of Colloidal Two-Dimensional Titanium Carbides (MXenes)," *Chemistry of Materials*, vol. 29, no. 11, pp. 4848–4856, Jun. 2017, doi: 10.1021/ACS.CHEMMATER.7B00745.

[47] X. Zhao *et al.*, "Antioxidants Unlock Shelf-Stable Ti_3C_2T (MXene) Nanosheet Dispersions," *Matter*, vol. 1, no. 2, pp. 513–526, Aug. 2019, doi: 10.1016/J.MATT.2019.05.020.

[48] B. Anasori, M. R. Lukatskaya, and Y. Gogotsi, "2D metal carbides and nitrides (MXenes) for energy storage," *Nat Rev Mater*, vol. 2, no. 2, Jan. 2017, doi: 10.1038/NATREVMATS.2016.98.

[49] B. Ahmed, D. H. Anjum, Y. Gogotsi, and H. N. Alshareef, "Atomic layer deposition of SnO_2 on MXene for Li-ion battery anodes," *Nano Energy*, vol. 34, pp. 249–256, Apr. 2017, doi: 10.1016/J.NANOEN.2017.02.043.

[50] Q. Xue*et al.*, "Photoluminescent Ti_3C_2MXene Quantum Dots for Multicolor Cellular Imaging," *Advanced Materials*, vol. 29, no. 15, p. 1604847, Apr. 2017, doi: 10.1002/ADMA.201604847.

[51] K. Zhong *et al.*, "A novel near-infrared fluorescent probe for highly selective recognition of hydrogen sulfide and imaging in living cells," *RSC Adv*, vol. 8, no. 42, pp. 23924–23929, Jun. 2018, doi: 10.1039/C8RA03457E.

[52] R. Thakur *et al.*, "Insights into the thermal and chemical stability of multilayered V_2CT_xMXene," *Nanoscale*, vol. 11, no. 22, pp. 10716–10726, Jun. 2019, doi: 10.1039/C9NR03020D.

[53] N. K. Chaudhari, H. Jin, B. Kim, D. San Baek, S. H. Joo, and K. Lee, "MXene: an emerging two-dimensional material for future energy conversion and storage applications," *J Mater Chem A Mater*, vol. 5, no. 47, pp. 24564–24579, Dec. 2017, doi: 10.1039/C7TA09094C.

[54] J. Come *et al.*, "Controlling the actuation properties of MXene paper electrodes upon cation intercalation," *Nano Energy*, vol. 17, pp. 27–35, 2015, doi: 10.1016/J.NANOEN.2015.07.028.

[55] J. N. Coleman *et al.*, "Two-dimensional nanosheets produced by liquid exfoliation of layered materials," *Science*, vol. 331, no. 6017, pp. 568–571, Feb. 2011, doi: 10.1126/SCIENCE.1194975.

[56] O. Mashtalir, M. Naguib, B. Dyatkin, Y. Gogotsi, and M. W. Barsoum, "Kinetics of aluminum extraction from Ti_3AlC_2 in hydrofluoric acid," *Mater Chem Phys*, vol. 139, no. 1, pp. 147–152, Apr. 2013, doi: 10.1016/J.MATCHEMPHYS.2013.01.008.

[57] M. Naguib *et al.*, "One-step synthesis of nanocrystalline transition metal oxides on thin sheets of disordered graphitic carbon by oxidation of MXenes," *Chemical Communications*, vol. 50, no. 56, pp. 7420–7423, Jun. 2014, doi: 10.1039/C4CC01646G.

[58] Y. Pei *et al.*, "$Ti_3C_2T_X$MXene for Sensing Applications: Recent Progress, Design Principles, and Future Perspectives," *ACS Nano*, vol. 15, no. 3, pp. 3996–4017, Mar. 2021, doi: 10.1021/ACSNANO.1C00248.

[59] A. Lipatov, M. Alhabeb, M. R. Lukatskaya, A. Boson, Y. Gogotsi, and A. Sinitskii, "MXene Materials: Effect of Synthesis on Quality, Electronic Properties and Environmental Stability of Individual Monolayer Ti_3C_2MXene Flakes (Adv. Electron. Mater. 12/2016)," *Adv Electron Mater*, vol. 2, no. 12, Dec. 2016, doi: 10.1002/AELM.201670068.

[60] F. Liu *et al.*, "Preparation of Ti3C2 and Ti2C MXenes by fluoride salts etching and methane adsorptive properties," *Appl Surf Sci*, vol. 416, pp. 781–789, Sep. 2017, doi: 10.1016/J.APSUSC.2017.04.239.

[61] X. Wang *et al.*, "A new etching environment (FeF_3/HCl) for the synthesis of two-dimensional titanium carbide MXenes: a route towards selective reactivity vs. water," *J Mater Chem A Mater*, vol. 5, no. 41, pp. 22012–22023, Oct. 2017, doi: 10.1039/C7TA01082F.

[62] M. Alhabeb*et al.*, "Guidelines for Synthesis and Processing of Two-Dimensional Titanium Carbide ($Ti_3C_2T_x$MXene)," *Chemistry of Materials*, vol. 29, no. 18, pp. 7633–7644, Sep. 2017, doi: 10.1021/ACS.CHEMMATER.7B02847.

[63] X. Zhang, Y. Yang, and Z. Zhou, "Towards practical lithium-metal anodes," *Chem Soc Rev*, vol. 49, no. 10, pp. 3040–3071, May 2020, doi: 10.1039/C9CS00838A.

[64] M. Mariano *et al.*, "Solution-processed titanium carbide MXene films examined as highly transparent conductors," *Nanoscale*, vol. 8, no. 36, pp. 16371–16378, Sep. 2016, doi: 10.1039/C6NR03682A.

[65] Y. Y. Peng *et al.*, "All-MXene (2D titanium carbide) solid-state microsupercapacitors for on-chip energy storage," *Energy Environ Sci*, vol. 9, no. 9, pp. 2847–2854, Aug. 2016, doi: 10.1039/C6EE01717G.

[66] L. Zhang *et al.*, "MXene coupled with molybdenum dioxide nanoparticles as 2D-0D pseudocapacitive electrode for high performance flexible asymmetric micro-supercapacitors," *Journal of Materiomics*, vol. 6, no. 1, pp. 138–144, Mar. 2020, doi: 10.1016/J.JMAT.2019.12.013.

[67] E. Quain*et al.*, "Direct Writing of Additive-Free MXene-in-Water Ink for Electronics and Energy Storage," *Adv Mater Technol*, vol. 4, no. 1, Jan. 2018, doi: 10.1002/ADMT.201800256.

[68] A. Lerf and R. Schöllhorn, "Solvation Reactions of Layered Ternary Sulfides A_xTiS_2, A_xNbS_2, and A_xTaS_2," *Inorg Chem*, vol. 16, no. 11, pp. 2950–2956, Nov. 1977, doi: 10.1021/IC50177A057/ASSET/IC50177A057.FP.PNG_V03.

[69] M. Ghidiu, J. Halim, S. Kota, D. Bish, Y. Gogotsi, and M. W. Barsoum, "Ion-Exchange and Cation Solvation Reactions in Ti_3C_2MXene," *Chemistry of Materials*, vol. 28, no. 10, pp. 3507–3514, May 2016, doi: 10.1021/ACS.CHEMMATER.6B01275/SUPPL_FILE/CM6B01275_SI_001.PDF.

[70] J. Xuan *et al.*, "Organic-Base-Driven Intercalation and Delamination for the Production of Functionalized Titanium Carbide Nanosheets with Superior Photothermal Therapeutic Performance," *Angew Chem Int Ed Engl*, vol. 55, no. 47, pp. 14569–14574, Nov. 2016, doi: 10.1002/ANIE.201606643.

[71] X. Yu, X. Cai, H. Cui, S. W. Lee, X. F. Yu, and B. Liu, "Fluorine-free preparation of titanium carbide MXene quantum dots with high near-infrared photothermal performances for cancer therapy," *Nanoscale*, vol. 9, no. 45, pp. 17859–17864, Dec. 2017, doi: 10.1039/C7NR05997C.

[72] T. Li *et al.*, "Fluorine-Free Synthesis of High-Purity $Ti_3C_2T_x$ (T=OH, O) via Alkali Treatment," *Angew Chem Int Ed Engl*, vol. 57, no. 21, pp. 6115–6119, May 2018, doi: 10.1002/ANIE.201800887.

[73] R. M. Ronchi, J. T. Arantes, and S. F. Santos, "Synthesis, structure, properties and applications of MXenes: Current status and perspectives," *Ceram Int*, vol. 45, no. 15, pp. 18167–18188, Oct. 2019, doi: 10.1016/J.CERAMINT.2019.06.114.

[74] B. Anasori, M. R. Lukatskaya, and Y. Gogotsi, "2D metal carbides and nitrides (MXenes) for energy storage," *Nat Rev Mater*, vol. 2, no. 2, Jan. 2017, doi: 10.1038/NATREVMATS.2016.98.

[75] M. Naguib, V. N. Mochalin, M. W. Barsoum, and Y. Gogotsi, "25th anniversary article: MXenes: a new family of two-dimensional materials," *Adv Mater*, vol. 26, no. 7, pp. 992–1005, Feb. 2014, doi: 10.1002/ADMA.201304138.

[76] J. C. Lei, X. Zhang, and Z. Zhou, "Recent advances in MXene: Preparation, properties, and applications," *Front Phys (Beijing)*, vol. 10, no. 3, pp. 276–286, Jun. 2015, doi: 10.1007/S11467-015-0493-X.

[77] L. Wang *et al.*, "Synthesis and electrochemical performance of $Ti_3C_2T_x$ with hydrothermal process," *Electronic Materials Letters*, vol. 12, no. 5, pp. 702–710, Sep. 2016, doi: 10.1007/S13391-016-6088-Z/METRICS.

[78] J. Pang *et al.*, "Applications of 2D MXenes in energy conversion and storage systems," *Chem Soc Rev*, vol. 48, no. 1, pp. 72–133, Jan. 2019, doi: 10.1039/C8CS00324F.

[79] M. R. Lukatskaya*et al.*, "Cation intercalation and high volumetric capacitance of two-dimensional titanium carbide," *Science*, vol. 341, no. 6153, pp. 1502–1505, 2013, doi: 10.1126/SCIENCE.1241488.

[80] M. Ghidiu, M. R. Lukatskaya, M. Q. Zhao, Y. Gogotsi, and M. W. Barsoum, "Conductive two-dimensional titanium carbide 'clay' with high volumetric capacitance," *Nature*, vol. 516, no. 7529, pp. 78–81, Dec. 2014, doi: 10.1038/NATURE13970.

[81] E. Kayali, A. Vahidmohammadi, J. Orangi, and M. Beidaghi, "Controlling the Dimensions of 2D MXenes for Ultrahigh-Rate Pseudocapacitive Energy Storage," *ACS Appl Mater Interfaces*, vol. 10, no. 31, pp. 25949–25954, Aug. 2018, doi: 10.1021/ACSAMI.8B07397.

[82] M. R. Lukatskaya*et al.*, "Ultra-high-rate pseudocapacitive energy storage in two-dimensional transition metal carbides," *Nat Energy*, vol. 6, Jul. 2017, doi: 10.1038/NENERGY.2017.105.

[83] J. Pang *et al.*, "Applications of 2D MXenes in energy conversion and storage systems," *Chem Soc Rev*, vol. 48, no. 1, pp. 72–133, Jan. 2019, doi: 10.1039/C8CS00324F.

[84] K. Hantanasirisakul and Y. Gogotsi, “Electronic and Optical Properties of 2D Transition Metal Carbides and Nitrides (MXenes),” *Adv Mater*, vol. 30, no. 52, Dec. 2018, doi: 10.1002/ADMA.201804779.

[85] V. Ming *et al.*, “Correction: Recent progress in layered transition metal carbides and/or nitrides (MXenes) and their composites: synthesis and applications,” *J Mater Chem A Mater*, vol. 5, no. 18, pp. 8769–8769, May 2017, doi: 10.1039/C7TA90088K.

[86] C. Eames and M. S. Islam, “Ion intercalation into two-dimensional transition-metal carbides: global screening for new high-capacity battery materials,” *J Am Chem Soc*, vol. 136, no. 46, pp. 16270–16276, Nov. 2014, doi: 10.1021/JA508154E.

[87] J. Zhu, A. Chroneos, J. Eppinger, and U. Schwingenschlögl, “S-functionalized MXenes as electrode materials for Li-ion batteries,” *Appl Mater Today*, vol. 5, pp. 19–24, Dec. 2016, doi: 10.1016/J.APMT.2016.07.005.

[88] Q. Tang, Z. Zhou, and P. Shen, “Are MXenes promising anode materials for Li-ion batteries? Computational studies on electronic properties and Li storage capability of Ti_3C_2 and $Ti_3C_2X_2$ (X = F, OH) monolayer,” *J Am Chem Soc*, vol. 134, no. 40, pp. 16909–16916, Oct. 2012, doi: 10.1021/JA308463R.

[89] Q. Tang, Z. Zhou, and P. Shen, “Are MXenes promising anode materials for Li-ion batteries? Computational studies on electronic properties and Li storage capability of Ti_3C_2 and $Ti_3C_2X_2$ (X = F, OH) monolayer,” *J Am Chem Soc*, vol. 134, no. 40, pp. 16909–16916, Oct. 2012, doi: 10.1021/JA308463R/SUPPL_FILE/JA308463R_SI_001.PDF.

[90] Z. Ling *et al.*, “Flexible and conductive MXene films and nanocomposites with high capacitance,” *Proc Natl Acad Sci U S A*, vol. 111, no. 47, pp. 16676–16681, Nov. 2014, doi: 10.1073/PNAS.1414215111.

[91] Q. Xue*et al.*, “Photoluminescent Ti3C2 MXene Quantum Dots for Multicolor Cellular Imaging,” *Advanced Materials*, vol. 29, no. 15, p. 1604847, Apr. 2017, doi: 10.1002/ADMA.201604847.

[92] A. Sinha *et al.*, “MXene: An emerging material for sensing and biosensing,” *TrAC Trends in Analytical Chemistry*, vol. 105, pp. 424–435, Aug. 2018, doi: 10.1016/J.TRAC.2018.05.021.

[93] X. F. Yu *et al.*, “Monolayer Ti2CO2: A Promising Candidate for NH3 Sensor or Capturer with High Sensitivity and Selectivity,” *ACS Appl Mater Interfaces*, vol. 7, no. 24, pp. 13707–13713, Jun. 2015, doi: 10.1021/ACSAMI.5B03737/SUPPL_FILE/AM5B03737_SI_001.PDF.

[94] B. Xiao, Y. C. Li, X. F. Yu, and J. B. Cheng, “MXenes: Reusable materials for NH3 sensor or capturer by controlling the charge injection,” *Sens Actuators B Chem*, vol. 235, pp. 103–109, Nov. 2016, doi: 10.1016/J.SNB.2016.05.062.

[95] Q. Xue*et al.*, "Photoluminescent Ti_3C_2MXene Quantum Dots for Multicolor Cellular Imaging," *Adv Mater*, vol. 29, no. 15, Apr. 2017, doi: 10.1002/ADMA.201604847.

[96] Q. Xue*et al.*, "Photoluminescent Ti_3CMXene Quantum Dots for Multicolor Cellular Imaging," *Advanced Materials*, vol. 29, no. 15, p. 1604847, Apr. 2017, doi: 10.1002/ADMA.201604847.

[97] B. Xu *et al.*, "Ultrathin MXene-Micropattern-Based Field-Effect Transistor for Probing Neural Activity," *Advanced Materials*, vol. 28, no. 17, pp. 3333–3339, May 2016, doi: 10.1002/ADMA.201504657.

[98] Q. Peng *et al.*, "Unique lead adsorption behavior of activated hydroxyl group in two-dimensional titanium carbide," *J Am Chem Soc*, vol. 136, no. 11, pp. 4113–4116, Mar. 2014, doi: 10.1021/JA500506K.

[99] Y. Ying *et al.*, "Two-dimensional titanium carbide for efficiently reductive removal of highly toxic chromium(VI) from water," *ACS Appl Mater Interfaces*, vol. 7, no. 3, pp. 1795–1803, Jan. 2015, doi: 10.1021/AM5074722.

[100] A. Shahzad *et al.*, "Two-Dimensional $Ti_3C_2T_x$MXene Nanosheets for Efficient Copper Removal from Water," *ACS Sustain Chem Eng*, vol. 5, no. 12, pp. 11481–11488, Dec. 2017, doi: 10.1021/ACSSUSCHEMENG.7B02695.

[101] Q. Zhang *et al.*, "Efficient phosphate sequestration for water purification by unique sandwich-like MXene/magnetic iron oxide nanocomposites," *Nanoscale*, vol. 8, no. 13, pp. 7085–7093, Mar. 2016, doi: 10.1039/C5NR09303A.

[102] O. Mashtalir, K. M. Cook, V. N. Mochalin, M. Crowe, M. W. Barsoum, and Y. Gogotsi, "Dye adsorption and decomposition on two-dimensional titanium carbide in aqueous media," *J Mater Chem A Mater*, vol. 2, no. 35, pp. 14334–14338, Sep. 2014, doi: 10.1039/C4TA02638A.

[103] A. Szuplewska*et al.*, "Future Applications of MXenes in Biotechnology, Nanomedicine, and Sensors," *Trends Biotechnol*, vol. 38, no. 3, pp. 264–279, Mar. 2020, doi: 10.1016/J.TIBTECH.2019.09.001.

[104] R. S. Riley and E. S. Day, "Gold nanoparticle-mediated photothermal therapy: applications and opportunities for multimodal cancer treatment," *Wiley Interdiscip Rev NanomedNanobiotechnol*, vol. 9, no. 4, Jul. 2017, doi: 10.1002/WNAN.1449.

[105] R. S. Riley and E. S. Day, "Gold nanoparticle-mediated photothermal therapy: applications and opportunities for multimodal cancer treatment," *Wiley Interdiscip Rev NanomedNanobiotechnol*, vol. 9, no. 4, Jul. 2017, doi: 10.1002/WNAN.1449.

[106] C. Dai, H. Lin, G. Xu, Z. Liu, R. Wu, and Y. Chen, "Biocompatible 2D Titanium Carbide (MXenes) Composite Nanosheets for pH-Responsive MRI-Guided Tumor Hyperthermia," *Chemistry of Materials*, vol. 29, no. 20, pp. 8637–8652, Oct. 2017, doi: 10.1021/ACS.CHEMMATER.7B02441/SUPPL_FILE/CM7B02441_SI_001.PDF.

[107] A. Szuplewska*et al.*, "Future Applications of MXenes in Biotechnology, Nanomedicine, and Sensors.," *Trends Biotechnol*, vol. 38, no. 3, pp. 264–279, Mar. 2020, doi: 10.1016/J.TIBTECH.2019.09.001.

[108] X. Yu, X. Cai, H. Cui, S. W. Lee, X. F. Yu, and B. Liu, "Fluorine-free preparation of titanium carbide MXene quantum dots with high near-infrared photothermal performances for cancer therapy," *Nanoscale*, vol. 9, no. 45, pp. 17859–17864, Nov. 2017, doi: 10.1039/C7NR05997C.

[109] S. Pan *et al.*, "2D MXene-Integrated 3D-Printing Scaffolds for Augmented Osteosarcoma Phototherapy and Accelerated Tissue Reconstruction," *Adv Sci (Weinh)*, vol. 7, no. 2, Jan. 2019, doi: 10.1002/ADVS.201901511.

[110] Y. Wang, Y. Xu, M. Hu, H. Ling, and X. Zhu, "MXenes: Focus on optical and electronic properties and corresponding applications," *Nanophotonics*, vol. 9, no. 7, pp. 1601–1620, Jul. 2020, doi: 10.1515/NANOPH-2019-0556/PDF.

[111] S. K. Nemani*et al.*, "High-Entropy 2D Carbide MXenes: $TiVNbMoC_3$ and $TiVCrMoC_3$," *ACS Nano*, vol. 15, no. 8, pp. 12815–12825, Aug. 2021, doi: 10.1021/ACSNANO.1C02775.

[112] Q. Tang, Z. Zhou, and P. Shen, "Are MXenes promising anode materials for Li ion batteries? Computational studies on electronic properties and Li storage capability of Ti_3C_2 and $Ti_3C_2X_2$ (X = F, OH) monolayer," *J Am Chem Soc*, vol. 134, no. 40, pp. 16909–16916, Oct. 2012, doi: 10.1021/JA308463R.

[113] T. Hu, J. Wang, H. Zhang, Z. Li, M. Hu, and X. Wang, "Vibrational properties of Ti_3C_2 and $Ti_3C_2T_2$ (T = O, F, OH) monosheets by first-principles calculations: a comparative study," *Physical Chemistry Chemical Physics*, vol. 17, no. 15, pp. 9997–10003, Apr. 2015, doi: 10.1039/C4CP05666C.

[114] O. Mashtalir*et al.*, "Intercalation and delamination of layered carbides and carbonitrides," *Nat Commun*, vol. 4, 2013, doi: 10.1038/NCOMMS2664.

[115] O. Mashtalir, M. R. Lukatskaya, M. Q. Zhao, M. W. Barsoum, and Y. Gogotsi, "Amine-Assisted Delamination of Nb_2C MXene for Li-Ion Energy Storage Devices," *Adv Mater*, vol. 27, no. 23, pp. 3501–3506, Jun. 2015, doi: 10.1002/ADMA.201500604.

[116] B. Xu *et al.*, "Achieving remarkable mechanochromism and white-light emission with thermally activated delayed fluorescence through the molecular heredity principle," *Chem Sci*, vol. 7, no. 3, pp. 2201–2206, Feb. 2016, doi: 10.1039/C5SC04155D.

[117] C. E. Shuck, K. Ventura-Martinez, A. Goad, S. Uzun, M. Shekhirev, and Y. Gogotsi, "Safe Synthesis of MAX and MXene: Guidelines to Reduce Risk During Synthesis," *ACS Chemical Health & Safety*, vol. 28, no. 5, pp. 326–338, Sep. 2021, doi: 10.1021/ACS.CHAS.1C00051.

[118] M. Naguib *et al.*, “Two-dimensional transition metal carbides,” *ACS Nano*, vol. 6, no. 2, pp. 1322–1331, Feb. 2012, doi: 10.1021/NN204153H.